Interacting fermions in synthetic non-Abelian gauge fields

Vijay B. Shenoy*, Jayantha P. Vyasanakere and Sudeep Kumar Ghosh

Centre for Condensed Matter Theory, Department of Physics, Indian Institute of Science, Bangalore 560 012, India

Generation and study of synthetic gauge fields has enhanced the possibility of using cold atom systems as quantum emulators of condensed matter Hamiltonians. In this article we describe the physics of interacting spin-$\frac{1}{2}$ fermions in synthetic non-Abelian gauge fields which induce a Rashba spin–orbit interaction on the motion of the fermions. We show that the fermion system can evolve to a Bose–Einstein condensate of a novel boson which we call *rashbon*. The rashbon–rashbon interaction is shown to be *independent* of the interaction between the constituent fermions. We also show that spin–orbit coupling can help enhancing superfluid transition temperature of weak superfluids to the order of Fermi temperature. A non-Abelian gauge field, when used in conjunction with another potential, can generate interesting Hamiltonians such as that of a magnetic monopole.

Keywords: Cold atom systems, fermions, rashbons, synthetic gauge fields.

QUANTUM condensed matter physics has played a pivotal role in the advancement of modern technology, particularly those relating to computing, information and communication. Indeed, it is the quantum mechanical theory of energy bands in solids that provided an understanding of semiconductors which in turn enabled the development of the transistor which ushered in the digital revolution. The ever insatiable societal demand for cheaper, smaller and faster devices has spurred the search for materials and systems with 'colossal responses'. Vivid examples of this is the discovery of high T_c cuprate superconductors[1], manganites exhibiting colossal magneto-resistance[2] and more recently interface electronic systems[3]. Not only have these breakthroughs held the promise of better devices and applications, they have captured the attention and energies of theorists ever since they made their appearance. This owes to a common feature of most of these novel materials – the presence of strong electronic interactions and correlations. Unlike the physics of materials like semiconductors and metals used in devices, the strongly correlated materials are much less understood from a theoretical point of view. The phases and excitations of such systems have refused to tow the line of established paradigms of condensed matter physics. There are debates, often heated, even on the simplest Hamiltonian needed for their essential description. This is compounded by the fact that even the simplest Hamiltonian that includes strong electron correlations such as the Hubbard model, has withstood theoretical assaults for several decades. Experiments, which therefore drive the theorists' intuition, are difficult owing to many factors such as controlled sample preparation and characterization. All of these aspects have colluded to effect the tardy pace at which the strongly correlated materials have found applications arising from the lack of theoretical inputs that guide their design. Yet there is a sense of expectant anticipation that condensed matter physics will, sooner than later, provide clues to producing room-temperature superconductors and quantum computers, both no less momentous in human evolution than the harnessing of fire, using strongly correlated systems and their exotic excitations.

The year 1995 marks a milestone with the realization of Bose–Einstein condensate (BEC) of alkali atoms by Cornell, Wieman and Ketterle – the three won the Nobel Prize in Physics in 2001. The condensation occurred at a temperature in the range of nanokelvins, where quantum effects become prominent. The route to the realization of such temperature itself is a fascinating account with notable contributions by Chu, Cohen-Tannoudji and Phillips, who were awarded the Nobel Prize earlier in 1997. Not only was the creation of BEC, the laboratory realization of a phenomenon theoretically predicted nearly 80 years before by Bose and Einstein, it was the beginning of a new discipline – cold atom physics. While the early pioneers of this field were from the atomic–molecular–optics (AMO) community, condensed matter physicists soon realized the tremendous potential of cold atom systems to help address their outstanding questions. The idea itself goes back to Feynmann who suggested on several occasions the use of one quantum system to emulate another[4,5]. This, in the main, consists of constructing a model system out of controllable constituents (atoms in the present case) that mimics the Hilbert space and Hamiltonian of the condensed matter system of interest. For example, motion of electrons in a crystal can be simulated using an 'optical lattice' which is an interference pattern of counter-propagating laser beams[6]. The periodic modulation of light intensity makes the atom 'feel' a

*For correspondence. (e-mail: shenoy@physics.iisc.ernet.in)

periodic potential akin to that felt by an electron in a crystal. Furthermore, the interaction between atoms can be controlled by a Feshbach resonance[7], which provides a key handle on mimicking the physics of systems of interest. The key advantage is that a given condensed matter Hamiltonian can be created, and its phase diagram can be obtained experimentally, overcoming difficulties encountered in real material systems brought about by disorder and other extraneous factors that intervene in uncovering the key physics. Construction of *cold atom quantum emulators* has therefore become a rapidly advancing area[8] with spectacular success in throwing light on many condensed matter problems which include Bardeen–Cooper–Schreiffer (BCS)–BEC crossover of fermions including effects of imbalance[9–12], determination of the phase diagram of the Bose–Hubbard model[13,14], simulation of frustrated classical magnetism[15], realizing the Fulde–Ferrell–Larkin–Ovchinnikov (FFLO) phase[16], etc. (see refs 6, 17 and 18 for details).

The great expectations held by cold atom systems to reveal the underlying physics of strongly correlated systems have been somewhat tempered by several roadblocks. Apart from the difficulties associated with observation and inference of the states created in cold atom systems, there are two prominent issues. First is that of entropy removal or 'cooling problem' that has prevented the attainment of the strongly correlated quantum regime, particularly in fermionic cold atom systems in optical lattices[19]. While there have been theoretical suggestions to overcome this issue[20], laboratory progress has been slow. A second issue facing cold atom systems is the simulation of electromagnetic response of materials. Also, interesting states that arise in strong magnetic fields such as the quantum Hall states[21] which hold the promise of realization of quantum computer, are hard to realize. This difficulty arises since the atoms are charge neutral, naturally raising the question of how one simulates a charged system using neutral constituents. The answer to this question is motivated by the observation that in the presence of an electromagnetic field, the mechanical momentum of a particle is modified by the gauge field that describes the electromagnetic field. The generation of a 'synthetic gauge field' therefore amounts to creating circumstances where the mechanical momentum of a particle is modified by a quantity which can be controlled, effectively mimicking the motion of the particle in a electromagnetic field.

Generation and study of synthetic gauge fields have seen spectacular progress in the past years[22–26]. Synthetic gauge fields are generated by coupling the internal degrees of freedom such as the hyperfine states of the atom by means of laser light. This is done in such a fashion that the coupled system has a set of low-lying states at each point in space, and the particle moves adiabatically in this manifold (much like in the well-known Stern–Gerlach experiment). The low energy states at each spatial point vary, and are unitarily related to each other. Motion of the particle confined to this low energy manifold modifies its mechanical momentum, and this emulates the presence of a gauge field (for a more detailed account, see the review by Dalibard *et al.*[27]). What is noteworthy is that this process allows the emulation of both Abelian and non-Abelian gauge fields. The former is achieved when the low energy manifold contains but one state, and the latter when there are more than one state in the low energy manifold. Vortex injection via a synthetic Abelian gauge field in a BEC was reported by Lin *et al.*[22]. The same group later reported how Bose condensation is affected by a non-Abelian gauge field[24], the results of which were predicted in earlier theory papers[28,29].

In this article, we summarize and consolidate our recent work[30–34] on interacting spin-$\frac{1}{2}$ fermions in synthetic non-Abelian gauge fields focusing on the conceptual and physical aspects, leaving the reader to refer to the papers cited above for details. We first give a brief summary of the physics of interacting spin-$\frac{1}{2}$ fermions in the absence of the non-Abelian gauge field – this serves as the background for our work. This is followed by a discussion of the two-body problem in the presence of a non-Abelian gauge field. Many-body ground states of interacting fermions in a non-Abelian gauge field are then discussed, followed by their collective excitations. We then go on to discuss possible experimental signatures of our predictions and describe the possibility of using a non-Abelian gauge field in conjunction with another potential to produce exotic Hamiltonians. It will emerge that our results not only predict a new type of bosonic condensate (called the *rashbon* condensate), but also provide clues to enhancing transition temperatures of fermionic systems with weak attraction, and suggest routes to constructing systems that can pave the way to realize a quantum computer using cold atoms.

While we do not attempt a comprehensive review of this very active field, we note here some of the concurrent works that appeared shortly after ours. Rashbon anisotropy[35], BCS–BEC crossover including the Zeeman field at zero temperature[36,37], Dresselhaus-like spin–orbit interaction[38,39] and spin–orbit coupling in lower dimensions and lattices[40–42] have been studied, and transition temperatures estimated[43]. These fast paced developments, including those in bosons have been reviewed[44]. Aspects of spin–orbit-coupled fermions were suggested earlier in other contexts[45,46], before our independent reports.

Interacting fermions and the BCS–BEC crossover

Consider a system of spin-$\frac{1}{2}$ fermions in three spatial dimensions (3D) with a number density ρ which defines the Fermi momentum k_F via $k_F^3 = 3\pi^2\rho$. In units where $\hbar$

and mass of the fermions are set to unity, the kinetic energy of the system is described by

$$\mathcal{H}_K = \int \mathrm{d}^3\boldsymbol{r}\, \psi_\sigma^\dagger(\boldsymbol{r})\left(\frac{\boldsymbol{P}^2}{2} - \mu\right)\psi_\sigma(\boldsymbol{r}), \tag{1}$$

where $\boldsymbol{P}$ is the momentum operator, and $\psi_\sigma^\dagger(\boldsymbol{r})$ ($\psi_\sigma(\boldsymbol{r})$) a fermion operator that creates (destroys) a σ-spin ($\sigma = \uparrow, \downarrow$) fermion at position $\boldsymbol{r}$ and μ is the chemical potential. There is a local attraction between fermions of opposite spin in the singlet channel which is described by a contact potential (which is but a model for the actual interaction potential between the fermions)

$$\mathcal{H}_\upsilon = \upsilon \int \mathrm{d}^3\boldsymbol{r}\, \psi_\uparrow^\dagger(\boldsymbol{r})\psi_\downarrow^\dagger(\boldsymbol{r})\psi_\downarrow(\boldsymbol{r})\psi_\uparrow(\boldsymbol{r}). \tag{2}$$

While the model described by the Hamiltonian $\mathcal{H} = \mathcal{H}_K + \mathcal{H}_\upsilon$ appears simple enough, one encounters ultraviolet divergences. This problem is overcome by regularizing the theory[47] by introducing an ultraviolet momentum cut-off Λ. The interaction parameter υ is treated as a 'bare' parameter, to be traded for another physical parameter. This physical parameter is the two-body scattering length a_s, which is obtained by solving a two-body problem (one each of $\uparrow$ and $\downarrow$ fermions) using the actual potential of interaction. It can then be shown that

$$\frac{1}{4\pi a_s} = \frac{1}{\upsilon} + \Lambda, \tag{3}$$

ensuring that the infrared scattering properties of the contact potential (with the finite cut-off) match those of the actual potential. Note that increasing $1/a_s$ corresponds to increasing the attractive interaction.

It is worth recording the physics of the two-body problem for future discussion. A key feature of three spatial dimensions is that any arbitrary attractive interaction between two particles will not be able to produce a bound state between them, i.e. when a_s is negative there is *no bound state* for the two fermions. At an attraction of a critical strength characterized by a divergent scattering length $(1/a_s) = 0$, a bound state forms, and for a positive scattering length a_s its binding energy is $1/a_s^2$.

What happens with a finite density ρ of fermions when the attraction goes from weak to strong? This question was answered in the work of Eagles[48] and Leggett[49]. For weak attraction ($a_s < 0$, $|k_F a_s| \ll 1$), the ground state is a superfluid described by BCS theory[50] with large overlapping Cooper pairs. The chemical potential of this BCS state is essentially unchanged from that of the noninteracting system, i.e. $\mu \approx E_F = (k_F^2/2)$. For strong attraction, the situation changes. The pairs become tightly bound and assume a bosonic identity (since they are made up of two fermions), and the ground state can be viewed as a BEC of these bosons. The chemical potential of such a system is determined by the binding energy of the two-body problem, i.e. by $\mu \sim -(1/2a_s^2)$. Thus increasing the attraction from weak to strong results in a BCS to BEC crossover (there is no phase transition in the process, and hence a crossover). The transition temperatures across the crossover were soon evaluated[51,52]. It was shown that the exponentially small transition temperature on the BCS side is enhanced to the order of T_F (= E_F with Boltzmann constant $k_B = 1$). Much of this physics has been experimentally realized in cold atoms and the detailed review of the state of knowledge can be found in a recent book[53]. The superfluid realized at the resonant (divergent) scattering length is one of those with highest known ratio of transition to Fermi temperatures[54], $T_c/T_F = 0.17$.

Spin-$\frac{1}{2}$ fermions in synthetic non-Abelian gauge fields

Consider a uniform SU(2) gauge field $\boldsymbol{A} = A_i^\nu \boldsymbol{\tau}^\nu \boldsymbol{e}_i$, where $\boldsymbol{\tau}^\nu$ are the Pauli matrices, e_i is a unit vector in the i-direction and repeated ν index is summed over. As noted earlier, the velocity (mechanical momentum) operator is modified as $\boldsymbol{P} \to \boldsymbol{P} - \boldsymbol{A}$, and the kinetic energy operator in presence of the gauge field becomes

$$\mathcal{H}_{GF} = \int \mathrm{d}^3\boldsymbol{r}\, \psi^\dagger(\boldsymbol{r})\left[\frac{1}{2}(P_i\mathbf{1} - A_i^\mu\boldsymbol{\tau}^\mu)(P_i\mathbf{1} - A_i^\nu\boldsymbol{\tau}^\nu)\right]\psi(\boldsymbol{r}), \tag{4}$$

where $\psi^\dagger(\boldsymbol{r}) = (\psi_\uparrow^\dagger(\boldsymbol{r})\ \psi_\downarrow^\dagger(\boldsymbol{r}))$, P_i is the i-component of $\boldsymbol{P}$ and $\mathbf{1}$ is the SU(2) identity. Gauge fields of relevance to experiments are of the form $A_i^\mu = \lambda_i \delta_i^\mu$, which we call generalized Rashba gauge fields. With this gauge field the kinetic energy becomes

$$\mathcal{H}_R = \int \mathrm{d}^3\boldsymbol{r}\, \psi^\dagger(\boldsymbol{r})\left[\frac{\boldsymbol{P}^2}{2}\mathbf{1} - \boldsymbol{P}_\lambda \cdot \boldsymbol{\tau}\right]\psi(\boldsymbol{r}), \tag{5}$$

with $\boldsymbol{P}_\lambda = \lambda_x P_x \boldsymbol{e}_x + \lambda_y P_y \boldsymbol{e}_y + \lambda_z P_z \boldsymbol{e}_z$,

which describes a generalized Rashba spin–orbit coupling, hence the name Rashba gauge field. A Rashba gauge field is described by the 'vector' $\boldsymbol{\lambda} = \lambda_x \boldsymbol{e}_x + \lambda_y \boldsymbol{e}_y + \lambda_z \boldsymbol{e}_z = \lambda\hat{\boldsymbol{\lambda}}$ (see Figure 1 *a*) with $\lambda = |\boldsymbol{\lambda}|$ being the strength of the gauge field or spin–orbit coupling. We note here some special gauge fields with high symmetry that will prove useful in the discussion below. The first is extreme prolate (EP) gauge field which has only one nonzero component of $\boldsymbol{\lambda}$, the second is the extreme oblate (EO)

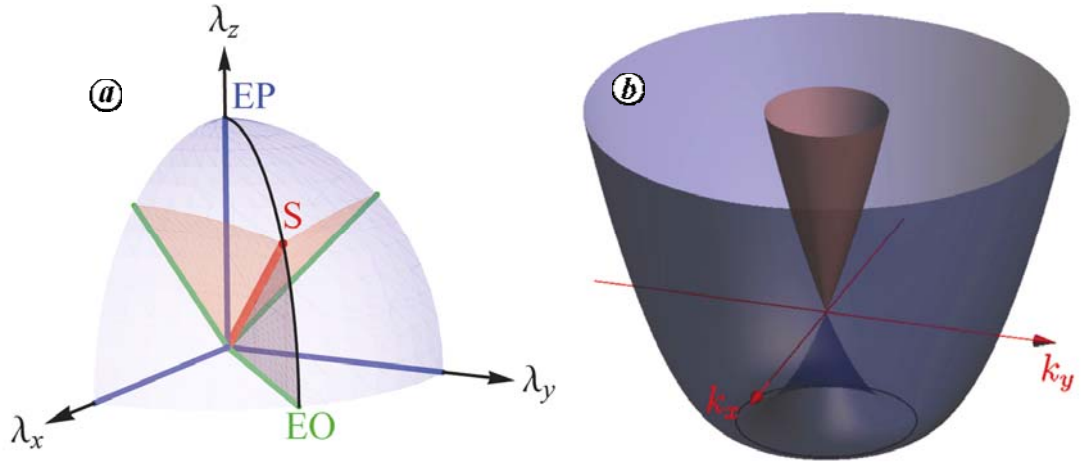

Figure 1. (***a***) Rashba gauge field configuration space. Points marked EP, S and EO represent the extreme prolate, spherical and extreme oblate gauge fields respectively. (***b***) Energy dispersion associated with the two helicities. For any given $\boldsymbol{k}$, the + helicity state (blue) has lower energy than the – helicity state (red). Note the lowest energy has a large number of degenerate states of the + helicity states at the bottom of the + helicity sheet (shown as a blue circle).

gauge field which has two nonzero component of $\boldsymbol{\lambda}$, e.g. $\boldsymbol{\lambda} = \lambda(\frac{1}{\sqrt{2}}, \frac{1}{\sqrt{2}}, 0)$ and third, the spherical (S) gauge field with $\boldsymbol{\lambda} = (\lambda/\sqrt{3})(1, 1, 0)$. Experimental suggestions for the generation of the EO gauge field have been made by Campbell *et al.*[55], and the S gauge field by Anderson *et al.*[56].

The one-particle states associated with the Rashba Hamiltonian eq. (5) are

$$|\boldsymbol{k}\alpha\rangle = |\boldsymbol{k}\rangle \otimes |\chi_\alpha(\boldsymbol{k})\rangle, \tag{6}$$

with energy $\varepsilon_{\boldsymbol{k}\alpha} = \frac{k^2}{2} - \alpha|\boldsymbol{k}_\lambda|$,

where $\boldsymbol{k}_\lambda$ is a vector defined similarly as $\boldsymbol{P}_\lambda$, $\alpha = \pm 1$ is the helicity, $|\boldsymbol{k}\rangle$ a plane wave state and $|\chi_\alpha(\boldsymbol{k})\rangle$ is a spin coherent state in the direction $\alpha\hat{\boldsymbol{k}}_\lambda$.

Interactions are now introduced via an attraction in the singlet channel as in eq. (2). Our research aims to uncover the physics of this system, i.e. interacting fermions in the presence of a Rashba gauge field. In particular, we study the evolution of the system of a given density of fermions and fixed attraction (given a_s) with increasing strength of the Rashba gauge coupling λ ($\hat{\boldsymbol{\lambda}}$ fixed). As in many dilute systems, the two-body problem holds the key, and this is what we studied first[30] and shall discuss now.

The two-body problem

We begin discussing the two-body problem with a discussion of the bound states of two spin-$\frac{1}{2}$ fermions in an EP gauge field. For this gauge field, at any given λ, there is no bound state for a negative scattering length ($a_s < 0$). A resonant scattering length $(1/a_{sc}) = 0$ is needed to force a bound state, and for a positive scattering length, the binding energy goes as $1/a_s^2$. This is identical to that obtained in the absence of the gauge field (which we call free vacuum). However, there is a key new aspect. The bound state wave function now contains both singlet and triplet pieces, which by itself is not surprising since a component of the spin itself is not a good quantum number for the problem owing to the spin–orbit interaction. What is interesting is that the triplet piece for this gauge field has the biaxial nematic spin structure similar to the B-phase[50] of ^{3}He.

Moving now to the EO gauge field (see Figure 1), we encounter a prima facie surprising result. We find that the critical attraction needed to form a bound state *vanishes*. Any attractive interaction induces a bound state leaving the critical scattering length $a_{sc} = 0^-$. For a small negative scattering length $|\lambda a_s| \ll 1$, the binding energy E_b is exponentially small ($E_b \approx (4\lambda^2/e^2)e^{\frac{-2\sqrt{2}}{\lambda|a_s|}}$). Notably the bound state wave function again has a triplet piece, this time similar to the uniaxial spin nematic structure associated with the A-phase of ^{3}He.

For the spherical (S) gauge field, we find again that the critical scattering length vanishes, i.e. $a_{sc} = 0^-$. What is interesting is that the binding energy for a small negative scattering length is algebraic in a_s, i.e., for $|\lambda a_s| \ll 1$, $E_b = (\lambda a_s/3)^2$. In fact, for this gauge field, we have obtained an analytical expression for the binding energy valid for any λ and a_s, i.e.

$$E_b = \frac{1}{4}\left(\frac{1}{a_s} + \sqrt{\frac{1}{a_s^2} + \frac{4\lambda^2}{3}}\right)^2.$$

The bound state wave function again has a triplet content with an isotropic structure.

For a generic Rashba gauge field $\boldsymbol{\lambda}$, we find that the critical scattering length is generically negative (see Figure 2). Thus a weaker attractive interaction will be able to produce a bound state of the two fermions in the presence of a Rashba gauge field – the Rashba gauge field acts as an 'attraction amplifier'. The physics behind the phenomenon can be traced to the infrared degeneracies induced by the Rashba gauge field. The density of states $g(\varepsilon)$, where ε is the energy measured from the band bottom, has the following behaviour. The density of states is unaffected by the gauge field at large energies, i.e. $g(\varepsilon) \sim \sqrt{\varepsilon}$ for $\varepsilon \gg \lambda^2$. The situation is very different in the infrared, i.e. for $\varepsilon \ll \lambda^2$, $g(\varepsilon) \approx \sqrt{\varepsilon}$ for the EP gauge field, $g(\varepsilon) \approx$ constant for EO, and $g(\varepsilon) \approx (1/\sqrt{\varepsilon})$ for the S gauge field. The gauge field drastically modifies the infrared density of states. In fact, the density of states is determined by the *co-dimension* of the one-particle ground state manifold. For example, for the S gauge field, the one-particle ground state manifold is a spherical surface (two-dimensional) of radius $\lambda/\sqrt{3}$, and its codimension is 1, and hence the density of states has a behaviour similar to that of free particles in 1D. It is this enhancement of the infrared density of states by the gauge field that promotes bound state formation, i.e. achieves the amplification of the attractive interaction.

We conclude the discussion of the two-body problem by considering the nature of the bound state in the presence of a gauge field when the scattering length is resonant, $(1/a_s) = 0$. The binding energy in this case is $E_b = \lambda^2 \mathcal{R}(\hat{\boldsymbol{\lambda}})$, where $\mathcal{R}$ is a positive dimensionless function of $\hat{\boldsymbol{\lambda}}$, except for the EP gauge field for which $\mathcal{R} = 0$. The bound state for this case is endowed with a characteristic triplet content η_t (the weight of the bound state wave function in the triplet sector). For example $\eta_t = 0.28$ and 1/4 for the EO and S gauge fields respectively. We will see that this bound state of the two fermions obtained at a resonant scattering length in the presence of a gauge field plays a crucial role in the physics of a finite density of interacting fermions in non-Abelian gauge fields, which we discuss next.

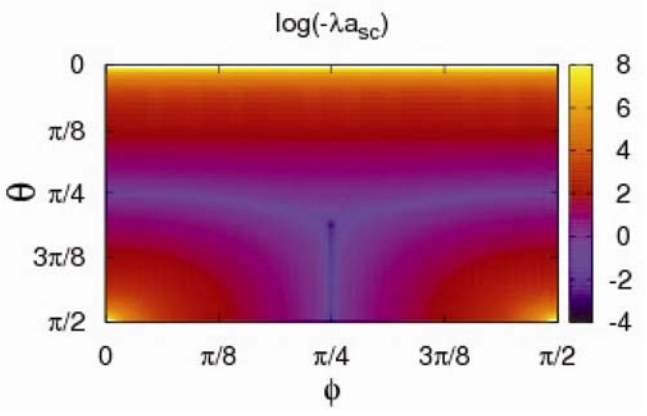

Figure 2. Critical scattering length as a function of $\hat{\boldsymbol{\lambda}}$ described by θ (polar) and ϕ (azimuthal) angles.

Ground state of interacting fermions in non-Abelian gauge fields

Before the introduction of interactions, it is useful to discuss the physics of a finite density ρ of *noninteracting* fermions in Rashba gauge fields. On increasing the strength of the gauge field (spin–orbit coupling) λ at fixed density, the chemical potential μ_{NI} of the noninteracting system changes. Analytical results can be obtained in two regimes. For the S gauge field,

$$\frac{\mu_{NI}(\lambda)}{E_F} \approx 1 - \frac{8}{3}\left(\frac{\lambda}{k_F}\right)^2, \quad \lambda \ll k_F, \tag{7}$$

and

$$\frac{\mu_{NI}(\lambda)}{E_F} \approx \left(\frac{k_F}{\lambda}\right)^4, \quad \lambda \gg k_F. \tag{8}$$

As is evident, there is a qualitative change in the behaviour of the noninteracting chemical potential with increasing λ. This can be traced to the change in the topology of the noninteracting Fermi surface with increasing λ, which occurs at a critical value λ_T (see Figure 3). The value of $\lambda_T = (\sqrt{3}/2^{2/3})k_F$ for the S gauge field is always of the order of k_F for any gauge field. When $\lambda = 0$, there are two spherical Fermi surfaces enclosing equal volumes (Figure 3 *a*). With increase of λ ($\lambda < \lambda_T$), the number of + helicity fermions increases with a corresponding decrease in the number of – helicity fermions, which results in the Fermi surfaces shown in Figure 3 *b*. At $\lambda = \lambda_T$, the – helicity Fermi surface vanishes, and for $\lambda \geq \lambda_T$ all particles are of + helicity. Interestingly, the topology of the + helicity Fermi surface changes at $\lambda = \lambda_T$. A single-sheet spherical Fermi surface for $\lambda < \lambda_T$ becomes two concentric spheres with enclosed states being occupied by fermions.

Turning on the interaction, we ask how does the ground state of a finite density ρ of fermions with a fixed attraction (a_s) evolve with increasing gauge coupling (spin–orbit interaction) λ? We focus on the case when the attraction is weak, i.e. $|k_F a_s| \ll 1$, $a_s < 0$, which contains the most interesting physics. The results of our mean field theory[31] for the evolution of the ground state are shown in Figure 4(I). For $\lambda \ll \lambda_T$, the chemical potential of the system is indistinguishable from that of the noninteracting system with the gauge field, and the pairing order parameter Δ is exponentially small and increases with increasing λ. After λ exceeds λ_T, a striking change occurs and the chemical potential smoothly crosses over

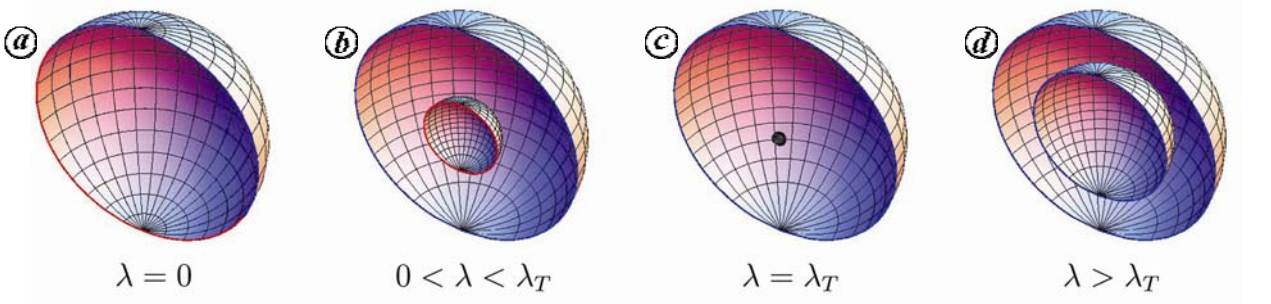

Figure 3. Transition in the topology of the Fermi surface of noninteracting fermions in a spherical gauge field with increasing λ. At $\lambda = \lambda_T$, the Fermi surface associated with the – helicity states vanishes (see (***c***)), and for $\lambda > \lambda_T$, the states enclosed between the two spherical surfaces (shown in (***d***)) are occupied and are all of + helicity. See text for further details.

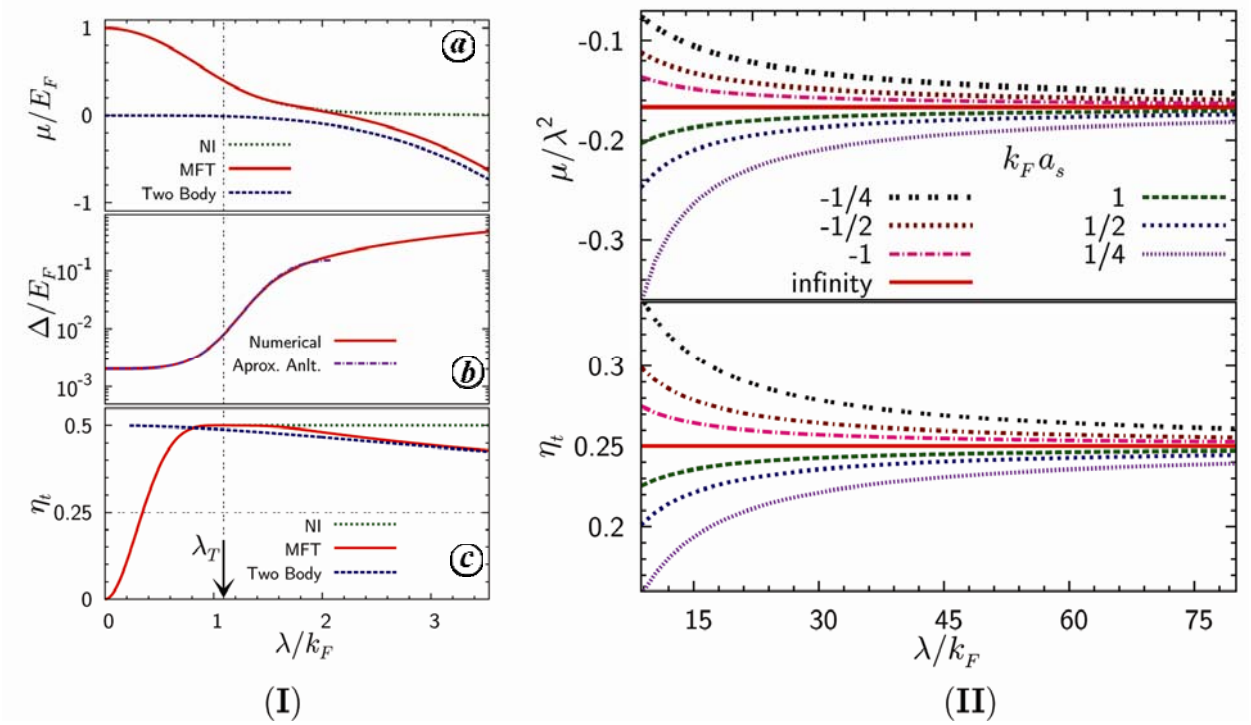

Figure 4. (I) BCS–BEC crossover induced by a spherical Rashba gauge field. (***a***) Dependence of chemical potential; (***b***) pairing order parameter Δ and (***c***) triplet content η_t on the strength λ of the Rashba gauge field with $k_F a_s = -1/4$. NI stands for noninteracting, MFT for mean field theory. (II) Evolution of chemical potential μ and triplet content η showing that the state attained at large λ is independent of the scattering length. This state is a Bose–Einstein condensate of rashbon, bosons whose properties are determined solely by the Rashba gauge field.

from the noninteracting value to that set by the two-body binding energy. What is even more noteworthy is that the triplet content η_t of the many-body pair wave function approaches the value of the triplet content of the two-body bound state wave function. All of these lead to the inescapable conclusion that *the Rashba gauge field engenders a crossover from a BCS-like state to a BEC state even for a weak attractive interaction*.

The natural question that follows this observation pertains to the nature of the BEC state obtained at large λ. Significantly, the BEC obtained for $\lambda \gg \lambda_T$ is a condensate of bosons whose properties are determined solely by the gauge field and not the scattering length between the fermions. This is evident from Figure 4(II) which shows that the chemical potential and triplet content tend to values that do not depend on the scattering length. A careful study shows that the bosonic state attained at large λ corresponds to the bound state of two fermions at resonant scattering length in the presence of the gauge field. As noted at the end of the discussion on the two-body problem, the properties of this state are determined solely by the Rashba gauge field. We have hence called this bosonic state as the rashbon. A Rashba gauge field therefore induces a crossover from a BCS state to a

rashbon-BEC state even for a weak attraction. For a positive scattering length, the gauge field induces a smooth crossover from the usual BEC to the rashbon BEC.

The emergence of the rashbon can also be understood by considering the mean field gap equation at large λ, where it reduces to the two-body secular equation. Since λ is the largest scale, we can use it to non-dimensionalize all other quantities in the gap equation leading to,

$$\frac{1}{4\pi\lambda a_s} = \frac{1}{2V}\sum_{\boldsymbol{k}\alpha}\left(\frac{1}{E-2\varepsilon_{\boldsymbol{k}\alpha}}+\frac{1}{k^2}\right), \tag{9}$$

where E is the dimensionless energy of the two-body state and the right-hand side here is completely dimensionless (for example, $\varepsilon_{\boldsymbol{k}\alpha}$ is measured in units of λ^2). The state obtained in the limit of $\lambda \to \infty$, is same as that obtained with $a_s \to \infty$ at fixed λ. This is the rashbon state.

Phase diagram

We now proceed to construct a qualitative phase diagram of interacting fermions in non-Abelian gauge fields in the a_s, λ, T space (T is temperature). This entails the estimation of the transition temperature T_c of the superfluid. We focus again on the regime with $|k_F a_s| \ll 1$. For, $\lambda \ll \lambda_T$, the superfluid state is a BCS-like state with weak pairing and the transition temperature is determined by the zero temperature paring gap. For the S gauge field, the transition temperature for $\lambda \ll \lambda_T$ is given by

$$T_c = \frac{e^{\gamma}}{\pi}\frac{8\mu_{NI}(\lambda)}{\exp\left(\dfrac{12\mu_{NI}(\lambda)}{6\mu_{NI}(\lambda)+\lambda^2}\right)} \times \exp\left(-\frac{3\pi\sqrt{\mu_{NI}(\lambda)}}{\sqrt{2}\,|a_s|\,(6\mu_{NI}(\lambda)+\lambda^2)}\right), \tag{10}$$

where $\gamma \approx 0.577$ is the Euler's constant.

In the regime $\lambda \gg \lambda_T$, the transition temperature is determined by the mass of the rashbons. We have carried out a detailed study[32] of the properties of rashbons, including the determination of their anisotropic mass tensor, triplet content, etc. For the S gauge field, the mass tensor is isotropic, with the rashbon mass (in units of the fermion mass)

$$m_R = \frac{3}{7}(4+\sqrt{2}) \approx 2.32. \tag{11}$$

Note that this is larger than the mass of the boson, which is exactly twice the fermion mass, obtained in the usual BEC in free vacuum with a small positive scattering length. The transition temperature of the rashbon BEC for the spherical gauge field can now be estimated to be $0.19T_F$. These considerations allow us to construct the phase diagram of the system shown in Figure 5 *a*. The most important aspect to be noted is that increasing the magnitude of *the spin–orbit interaction induced by the non-Abelian gauge field enhances the exponentially small transition temperature of the 'weak' superfluid to the order of Fermi temperature*.

We have also made a detailed study of the rashbon dispersion, i.e. its energy as a function of its centre of mass momentum $\boldsymbol{q}$. For $|\boldsymbol{q}| \ll \lambda$, the dispersion has the form

$$E(\boldsymbol{q}) = -E_R + \sum_i \frac{q_i^2}{2m_R^i}, \tag{12}$$

where E_R is the rashbon binding energy and m_R^i is the anisotropic rashbon mass introduced above. A remarkable feature discovered was that the bound state ceases to exist for centre of mass momenta larger than a critical value q_c. This critical value is always of the order of λ; for the spherical gauge field $q_c = (2/\sqrt{3})\lambda$. In fact, for $|\boldsymbol{q}| \gg q_c$, a positive scattering length is needed to induce a bound state of two fermions. Thus, the gauge field which acts as an attraction amplifier for small centre of mass momentum, plays the opposite role and inhibits bound state formation at larger centre of mass momenta. This finding is not just of academic interest, but has profound experimental consequences. In particular, we note that in systems with weak attraction, a strong pseudogap regime (see Figure 5 *b*) can be expected when $\sqrt{T} \approx k_F \approx \lambda$. This arises from the fact that state will be a soup of helical fermions and uncondensed rashbons arising from the physics just discussed.

Collective excitations and properties of rashbon condensates

We now turn to the discussion of collective excitations of the low temperature superfluid which we have studied using Gaussian fluctuation theory within a functional integral framework[34]. Our theory is capable of describing any Rashba gauge field. The excitations of a superfluid can be conveniently described in terms of phase and amplitude modes. The phase mode, characterized by the phase stiffness K^S, is gapless (Goldstone theorem), while the amplitude mode (or the Anderson–Higgs mode) is gapped with a 'mass' M_{AH}. The phase stiffness in free vacuum $K_0^S = \frac{\rho}{4}$ is independent of the scattering length owing to the Galilean invariance of the free vacuum system.

Figure 6 *a* shows the dependence of the phase stiffness on the strength of the spherical gauge field. The phase stiffness at any non-zero value of λ is lower than K_0^S, and has a non-monotonic behaviour with increasing λ. Similar

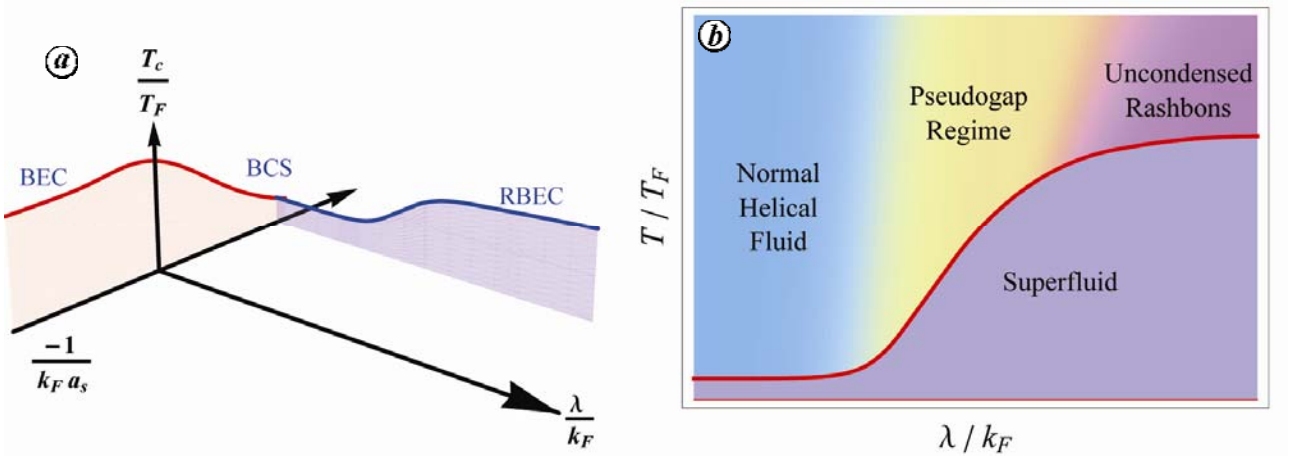

Figure 5. (***a***) 'Phase diagram' of interacting fermions in a Rashba gauge field. Note the enhancement of the transition temperature of a weak BCS superfluid to values of order T_F. The zero temperature condensate attained at large λ is independent of a_s and is the rashbon BEC. (***b***) Schematic showing possibility of strong pseudogap features in systems with weak attraction in the regime $\lambda \approx k_F \approx \sqrt{T}$.

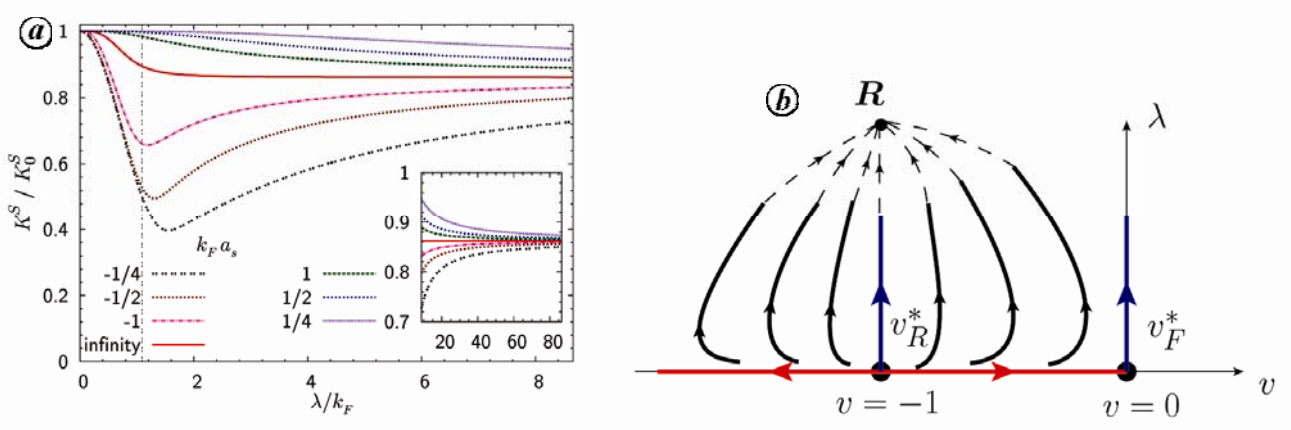

Figure 6. (***a***) Dependence of phase stiffness K^S on λ for various a_s in spherical gauge field. $K_0^S = (\rho/4)$ is the phase stiffness when $\lambda = 0$. (Inset) Demonstration of the emergent Galilean invariance at large λ by showing that K^S will tend to a value determined by rashbon mass, independent of a_s. (***b***) Schematic renormalization group flow diagram of the two-body problem.

result was reported earlier for the EO gauge field by Zhou and Zhang[57], which attributed this to the breaking of Galilean invariance due to the presence of the non-Abelian gauge field. We showed[34] that the superfluid obtained at large λ, i.e. the rashbon BEC has an emergent Galilean invariance and its phase stiffness tensor is given by

$$K_{ij}^{\mathrm{S}}(\lambda \to \infty) = \frac{\rho}{2}\frac{1}{m_i^{\mathrm{R}}}\delta_{ij}, \tag{13}$$

a result that is completely consistent with Leggett's theorem for Galilean invariant systems[58]. This result is graphically depicted in the inset of Figure 6 *a*. The mass of the Anderson–Higgs mode M_{AH} in the rashbon BEC is proportional to λ^2; for the S gauge field $M_{\mathrm{AH}} \approx \frac{2}{3}\lambda^2$.

That the rashbon BEC has a non-zero phase stiffness implies that the rashbons must be interacting. By a study of the sound mode[34], we showed that the rashbon BEC can be described by a theory of anisotropically dispersing bosons (see eq. (12)) interacting via a contact attraction. The rashbon–rashbon scattering length a_{R} was shown to be of the form $(N(\hat{\boldsymbol{\lambda}})/\lambda)$, where N is a dimensionless function dependent solely on $\hat{\boldsymbol{\lambda}}$. For the S gauge field, the rashbon–rashbon scattering length is

$$a_{\mathrm{R}} = \frac{3\sqrt{3}(4+\sqrt{2})}{7}\frac{1}{\lambda}. \tag{14}$$

Interestingly, the rashbon–rashbon scattering length is *independent* of the fermion–fermion scattering length a_s. To the best of the authors' knowledge, this is the first instance in a condensed matter system where the interaction between the emergent bosonic excitations (rashbons) is determined solely by a parameter that enters the kinetic energy of the constituent fermions.

The overall physics of interacting fermions in Rashba gauge fields is captured by the schematic RG flow diagram of the two-body problem shown in the υ–λ plane (see Figure 6 *b*). There are three fixed points, υ_F^*, υ_R^* and $\boldsymbol{R}$, which describe respectively the free, resonant and rashbon fixed points. When $\lambda = 0$, an interaction with $|\upsilon| < |\upsilon_R^*|$ flows back to the free fixed point, while an interaction $|\upsilon| > |\upsilon_R^*|$ flows away. Physically this means that a critical attraction is necessary for the formation of a bound state in free vacuum. Spin–orbit coupling is a relevant operator at both the fixed points υ_F^* and υ_R^*, and every point flows to the rashbon fixed point. The physics of a finite density of fermions at large λ is therefore controlled by the rashbon fixed point – we obtain a BEC of weakly interacting rashbons whose interactions are independent of the interactions between the constituent fermions.

Experimental signatures and other exciting possibilities with non-Abelian gauge fields

Consider a cloud of non-interacting fermions in an isotropic harmonic trap. Suppose we turn on a non-Abelian gauge field (increase λ) in an adiabatic fashion, what would one observe? Would there be a change in the size or shape of the cloud? We have shown[33] that for a generic gauge field the cloud *shrinks* with increasing λ. Our approach has been to use the local density approximation in which we use the equation of state of a homogeneous system. There are two regimes of λ which are set by the trap centre density. When λ exceeds a critical value determined by the trap centre density of the free vacuum system, the local Fermi surface at the centre of the trap undergoes a topology transition. For values of λ greater than this critical value, the cloud shrinks in a characteristic power law fashion

$$\frac{R}{R_0} = \left(\frac{k_F^0}{\lambda}\right)^{\varsigma}, \tag{15}$$

where R is the radius of the cloud, R_0 the radius of the cloud when $\lambda = 0$, k_F^0 the Fermi momentum determined by the trap centre density (with $\lambda = 0$) and ς is a characteristic exponent that depends on the particular gauge field. For the S gauge field, $\varsigma = \frac{1}{2}$. The physics of this owes to the lowering of mechanical momentum in the presence of the gauge field with a concomitant reduction of pressure[33]. In the presence of interactions, the cloud will shrink further due to the bound state formation, and eq. (15) provides an upper bound for the cloud size. We have also studied the validity of the local density approximation by comparing it with the result of exact numerical diagonalization[33] and found that while being qualitatively correct, it misses certain characteristic anisotropies of the cloud shape.

We now discuss novel possibilities with non-Abelian gauge fields in conjunction with another potential. Consider a spherically symmetric Harmonic trapping potential with a frequency ω_0. The one-particle Hamiltonian in the momentum representation is

$$\mathcal{H} = \frac{P^2}{2} - \boldsymbol{P}_\lambda \cdot \boldsymbol{\tau} - \frac{\omega_0^2}{2}\frac{\partial^2}{\partial \boldsymbol{P}^2}, \tag{16}$$

where we have used eq. (5) and the momentum representation of the position operator $\boldsymbol{r} = i(\partial/\partial \boldsymbol{P})$. Note that the potential operator does not commute with the spin–orbit coupling term, and hence helicity is not a good quantum number. However, for parameters such that $\omega_0 \ll \lambda^2$, helicity is 'approximately preserved' and we can make an adiabatic ansatz for the wave function as

$$|\psi\rangle = \int \mathrm{d}\boldsymbol{p}\phi(\boldsymbol{p})\,|\,\boldsymbol{p}\rangle \otimes |\,\chi_+(\boldsymbol{p})\rangle, \tag{17}$$

where $\phi(\boldsymbol{p})$ is a wave function in momentum space. The effective Hamiltonian[59] for this adiabatic wave function is

$$\mathcal{H}_{\text{eff}} = \frac{\omega_0^2}{2}\left(i\frac{\partial}{\partial \boldsymbol{p}} - \boldsymbol{A}\right)^2 + \varepsilon_+(\boldsymbol{p}) + V_{\text{BO}}(\boldsymbol{p}),$$

$$\boldsymbol{A} = -i\left\langle \chi_+(\boldsymbol{p}) \middle| \frac{\partial \chi_+(\boldsymbol{p})}{\partial \boldsymbol{p}} \right\rangle,$$

$$V_{\text{BO}}(\boldsymbol{p}) = \frac{\omega_0^2}{2}\left(\begin{array}{l}\left\langle \dfrac{\partial \chi_+(\boldsymbol{p})}{\partial p_i} \middle| \dfrac{\partial \chi_+(\boldsymbol{p})}{\partial p_i} \right\rangle - \left\langle \dfrac{\partial \chi_+(\boldsymbol{p})}{\partial p_i} \right| \\ \times \chi_+(\boldsymbol{p}) \Big\rangle \Big\langle \chi_+(\boldsymbol{p}) \Big| \dfrac{\partial \chi_+(\boldsymbol{p})}{\partial p_i} \Big\rangle \end{array}\right), \tag{18}$$

which in turn generates a new gauge field $\boldsymbol{A}$ that arises from the Pancharatnam–Berry phase, and a Born-Oppenheimer potential V_{BO}. For the spherical gauge field, the effective Hamiltonian expressed in spherical polar coordinates in momentum space (p, θ, ϕ) is

$$\begin{aligned}\mathcal{H}_{\text{eff}} = &-\frac{\omega_0^2}{2}\left(\frac{1}{p^2}\frac{\partial}{\partial p}p^2\frac{\partial}{\partial p}\right) \\ &+ \frac{\omega_0^2}{2p^2}\left[-\frac{1}{\sin\theta}\frac{\partial}{\partial\theta}\sin\theta\frac{\partial}{\partial\theta} + \left(Q\cot\theta + \frac{i}{\sin\theta}\frac{\partial}{\partial\phi}\right)^2\right] \\ &+ \frac{\omega_0^2}{4p^2} + \left(\frac{p^2}{2} - \frac{\lambda}{\sqrt{3}}p\right),\end{aligned} \tag{19}$$

where $Q = \frac{1}{2}$. This corresponds to a Hamiltonian[21] with a monopole at the origin in momentum space. The key

point to be noted is that a non-Abelian gauge field with judiciously designed potential $V(\boldsymbol{r})$ can produce Hamiltonians of interest to condensed matter physics.

Conclusion

In this article, we have described some of the rich physics that can be explored using non-Abelian synthetic gauge fields in fermionic systems. Non-Abelian gauge fields that induce a spin–orbit interaction promote bound-state formation of two particles even for weak attractions. They induce topological transitions of the noninteracting Fermi surface and this suggests a regime of novel BCS–BEC crossover. Even for a weak attraction, increasing the strength of a non-Abelian gauge field induces a crossover from a BCS state to a BEC state. The BEC obtained for large gauge coupling is a condensate of rashbons – novel fermionic bound pairs whose properties are determined solely by the gauge field. The rashbon–rashbon interaction is essentially independent of the interaction between the fermions – this is truly a novel state in this sense. Another key aspect is that the exponentially small transition temperature of a weak BCS superfluid can be strongly enhanced by spin–orbit interaction. These systems have a regime with interesting novel states where pseudogap effects are predicted. Use of non-Abelian gauge fields in conjunction with another suitably designed potential has the future possibility of generating many interesting Hamiltonians, possibly for realizing a quantum computer.

Much remains to be explored in this area. In particular, the regime where $\lambda \approx k_F$ is yet to be fully understood theoretically. This is also the regime that should be accessed experimentally. We do hope that our predictions of rashbon BEC, and promise of interesting pseudogap physics, etc. will motivate experimentalists. On a longer term, we hope that the lesson learnt regarding superfluidity, particularly regarding the enhancement of the transition temperature, will stimulate researchers to design materials which mimic this physics.

1. Lee, P. A., Nagaosa, N. and Wen, X.-G., Doping a Mott insulator: physics of high temperature superconductivity. *Rev. Mod. Phys*., 2006, **78**, 17–85.
2. Salamon, M. B. and Jaime, M., The physics of manganites: structure and transport. *Rev. Mod. Phys*., 2001, **73**, 583–628.
3. Mannhart, J. and Schlom, D. G., Oxide interfaces – an opportunity for electronics. *Science*, 2010, **327**, 1607–1611.
4. Trabesinger, A., Quantum simulation. *Nature Phys*., 2012, **8**, 263.
5. Cirac, J. I. and Zoller, P., Goals and opportunities in quantum simulation. *Nature Phys*., 2012, **8**, 264–266.
6. Bloch, I., Dalibard, J. and Zwerger, W., Many-body physics with ultracold gases. *Rev. Mod. Phys*., 2008, **80**, 885–964.
7. Chin, C., Grimm, R., Julienne, P. and Tiesinga, E., Feshbach resonances in ultracold gases. *Rev. Mod. Phys*., 2010, **82**, 1225–1286.
8. Bloch, I., Dalibard, J. and Nascimbene, S., Quantum simulations with ultracold quantum gases. *Nature Phys*., 2012, **8**, 267–276.
9. Regal, C. A., Greiner, M. and Jin, D. S., Observation of resonance condensation of fermionic atom pairs. *Phys. Rev. Lett*., 2004, **92**, 040403.
10. Partridge, G. B., Li, W., Liao, Y. A., Hulet, R. G., Haque, M. and Stoof, H. T. C., Deformation of a trapped Fermi gas with unequal spin populations. *Phys. Rev. Lett*., 2006, **97**, 190407.
11. Yong-il Shin, Schunck, C. H., Schirotzek, A. and Ketterle, W., Phase diagram of a two component Fermi gas with resonant interactions. *Nature*, 2006, **451**, 689–693.
12. Ketterle, W. and Zwierlein, M. W., Making, probing and understanding ultracold Fermi gases. *Nuovo Cimento Riv. Ser*., 2008, **31**, 247–422.
13. Gemelke, N., Zhang, X., Hung, C.-L. and Chin, C., *In situ* observation of incompressible Mott-insulating domains in ultracold atomic gases. *Nature*, 2009, **460**, 995–998.
14. Bakr, W. S. *et al.*, Probing the superfluid to Mott insulator transition at the single-atom level. *Science*, 2010, **329**, 547–550.
15. Struck, J. *et al.*, Quantum simulation of frustrated classical magnetism in triangular optical lattices. *Science*, 2011, **333**, 996–999.
16. Liao, Y.-A., Rittner, A. S. C., Paprotta, T., Li, W., Partridge, G. B., Hulet, R. G., Baur, S. K. and Mueller, E. J., Spin-imbalance in a one-dimensional Fermi gas. *Nature*, 2010, **467**, 567–569.
17. Giorgini, S., Pitaevskii, L. P. and Stringari, S., Theory of ultracold atomic Fermi gases. *Rev. Mod. Phys*., 2008, **80**, 1215–1274.
18. Esslinger, T., Fermi–Hubbard physics with atoms in an optical lattice. *Annu. Rev. Condensed Matter Phys*., 2010, **1**, 129–152.
19. McKay, D. C. and DeMarco, B., Cooling in strongly correlated optical lattices: prospects and challenges. *Rep. Prog. Phys*., 2011, **74**, 054401.
20. Ho, T.-L. and Zhou, Q., Squeezing out the entropy of fermions in optical lattices. *Proc. Natl. Acad. Sci. USA*, 2009, **106**, 6916–6920.
21. Jain, J. K., *Composite Fermions*, Cambridge University Press, Cambridge, UK, 2007.
22. Lin, Y.-J., Compton, R. L., Jimenez-Garcia, K., Porto, J. V. and Spielman, I. B., Synthetic magnetic fields for ultracold neutral atoms. *Nature*, 2009, **462**, 628–632.
23. Lin, Y.-J., Compton, R. L., Perry, A. R., Phillips, W. D., Porto, J. V. and Spielman, I. B., Bose–Einstein condensate in a uniform light-induced vector potential. *Phys. Rev. Lett*., 2009, **102**, 130401.
24. Lin, Y.-J., Jimenez-Garcia, K. and Spielman, I. B., Spin–orbit-coupled Bose–Einstein condensates. *Nature*, 2011, **471**, 83–86.
25. Wang, P. *et al.*, Spin–orbit coupled degenerate Fermi gases. 2012, ArXiv e-prints 1204.1887.
26. Cheuk, L. W., Sommer, A. T., Hadzibabic, Z., Yefsah, T., Bakr, W. S. and Zwierlein, M. W., Spin-injection spectroscopy of a spin–orbit coupled Fermi gas. 2012, ArXiv e-prints 1205.3483.
27. Dalibard, J., Gerbier, F., Juzeliūnas, G. and Öhberg, P., Colloquium: artificial gauge potentials for neutral atoms. *Rev. Mod. Phys*., 2011, **83**, 1523–1543.
28. Wang, C., Gao, C., Jian, C.-M. and Zhai, H., Spin–orbit coupled spinor Bose–Einstein condensates. *Phys. Rev. Lett*., 2010, **105**, 160403.
29. Ho, T.-L. and Zhang, S., Bose–Einstein condensates with spin–orbit interaction. *Phys. Rev. Lett*., 2011, **107**, 150403.
30. Vyasanakere, J. P. and Shenoy, V. B., Bound states of two spin-$\frac{1}{2}$ fermions in a synthetic non-Abelian gauge field. *Phys. Rev. B*, 2011, **83**, 094515.
31. Vyasanakere, J. P., Zhang, S. and Shenoy, V. B., BCS–BEC crossover induced by a synthetic non-Abelian gauge field. *Phys. Rev. B*, 2011, **84**, 014512.
32. Vyasanakere, J. P. and Shenoy, V. B., Rashbons: properties and their significance. *New J. Phys*., 2012, **14**, 043041.
33. Ghosh, S. K., Vyasanakere, J. P. and Shenoy, V. B., Trapped fermions in a synthetic non-Abelian gauge field. *Phys. Rev. A*, 2011, **84**, 053629.
34. Vyasanakere, J. P. and Shenoy, V. B., Collective excitations across the BCS–BEC crossover induced by a synthetic Rashba spin–orbit coupling. 2012, ArXiv e-prints 1201.5332.

35. Hu, H., Jiang, L., Liu, X.-J. and Pu, H., Probing anisotropic superfluidity in atomic Fermi gases with rashba spin–orbit coupling. *Phys. Rev. Lett.*, 2011, **107**, 195304.
36. Gong, M., Tewari, S. and Zhang, C., BCS–BEC crossover and topological phase transition in 3D spin–orbit coupled degenerate Fermi gases. *Phys. Rev. Lett.*, 2011, **107**, 195303.
37. Iskin, M. and Subaş ı, A. L., Stability of spin–orbit coupled Fermi gases with population imbalance. *Phys. Rev. Lett.*, 2011, **107**, 050402.
38. Han, L. and Sá de Melo, C. A. R., Evolution from BCS to BEC superfluidity in the presence of spin–orbit coupling. *Phys. Rev. A*, 2012, **85**, 011606.
39. Takei, S., Lin, C.-H., Anderson, B. M. and Galitski, V., Low-density molecular gas of tightly bound Rashba–Dresselhaus fermions. *Phys. Rev. A*, 2012, **85**, 023626.
40. Goldman, N., Kubasiak, A., Bermudez, A., Gaspard, P., Lewenstein, M. and Martin-Delgado, M. A., Non-Abelian optical lattices: anomalous quantum Hall effect and Dirac fermions. *Phys. Rev. Lett.*, 2009, **103**, 035301.
41. He, L. and Huang, X.-G., BCS–BEC crossover in 2D Fermi gases with Rashba spin–orbit coupling. *Phys. Rev. Lett.*, 2012, **108**, 145302.
42. Chen, G., Gong, M., Jia, S. and Zhang, C., BKT transition and Majorana fermions in 2D spin–orbit coupled Fermi superfluids. 2012, ArXiv e-prints 1201.2238.
43. Yu, Z.-Q. and Zhai, H., Spin–orbit coupled Fermi gases across a Feshbach resonance. *Phys. Rev. Lett.*, 2011, **107**, 195305.
44. Zhai, H., Spin–orbit coupled quantum gases. *Int. J. Mod. Phys. B*, 2012, **26**, 1230001.
45. Chaplik, A. V. and Magarill, L. I., Bound states in a two-dimensional short range potential induced by the spin–orbit interaction. *Phys. Rev. Lett.*, 2006, **96**, 126402.
46. Cappelluti, E., Grimaldi, C. and Marsiglio, F., Topological change of the Fermi surface in low-density Rashba gases: application to superconductivity. *Phys. Rev. Lett.*, 2007, **98**, 167002.
47. Braaten, E., Kusunoki, M. and Zhang, D., Scattering models for ultracold atoms. *Ann. Phys.*, 2008, **323**, 1770–1815.
48. Eagles, D. M., Possible pairing without superconductivity at low carrier concentrations in bulk and thin-film superconducting semiconductors. *Phys. Rev.*, 1969, **186**, 456–463.
49. Leggett, A. J., In *Modern Trends in the Theory of Condensed Matter* (eds Pekalski, A. and Przystawa, R.), Springer-Verlag, Berlin, 1980.
50. Leggett, A. J., *Quantum Liquids: Bose Condensation and Cooper Pairing in Condensed-Matter Systems*, Oxford University Press, 2006.
51. Noziéres, P. and Schmitt-Rink, S., Bose condensation in an attractive fermion gas: from weak to strong coupling superconductivity. *J. Low Temp. Phys.*, 1985, **59**, 195–211.
52. Randeria, M., In *Bose–Einstein Condensation* (eds Griffin, A., Snoke, D. and Stringari, S.), Cambridge University Press, 1995, Chapter 15.
53. Zwerger, W. (ed.), *The BCS–BEC Crossover and the Unitary Fermi Gas*, Vol. 836 of Lecture Notes in Physics, Springer-Verlag, Berlin, 2012.
54. Ku, M. J. H., Sommer, A. T., Cheuk, L. W. and Zwierlein, M. W., Revealing the superfluid lambda transition in the universal thermodynamics of a unitary Fermi gas. *Science*, 2012, **335**, 563–567.
55. Campbell, D. L., Juzeliūnas, G. and Spielman, I. B., Realistic Rashba and Dresselhaus spin–orbit coupling for neutral atoms. *Phys. Rev. A*, 2011, **84**, 025602.
56. Anderson, B. M., Juzeliūnas, G., Spielman, I. B. and Galitski, V. M., Synthetic 3D spin–orbit coupling. 2011, ArXiv e-prints 1112.6022.
57. Zhou, K. and Zhang, Z., Opposite effect of spin–orbit coupling on condensation and superfluidity. *Phys. Rev. Lett.*, 2012, **108**, 025301.
58. Leggett, A. J., On the superfluid fraction of an arbitrary many-body system at $T = 0$. *J. Stat. Phys.*, 1998, **93**, 927–941.
59. Moody, J., Shapere, A. and Wilczek, F., In *Geometric Phases in Physics* (eds Shapere, A. and Wilczek, F.), World Scientific, Singapore, 1989, pp. 160–183.

ACKNOWLEDGEMENTS. V.B.S. is grateful to DST, India (Ramanujan grant), DAE, India (SRC grant) and IUSSTF for generous support. J.V. and S.K.G. thankfully acknowledge support from CSIR, India via JRF grants.